A GIS-based map of the Hg-impacted area in the Paglia River basin (Monte Amiata Mining District – Italy): An operational instrument for

Journal of Geochemical Exploration

A GIS-based map of the Hg-impacted area in the Paglia River basin (Monte Amiata Mining District – Italy): an operational instrument for local authorities

--Manuscript Draft--

Manuscript Number:	
Article Type:	Research Paper
Keywords:	mercury; Monte Amiata; environmental management; contamination; geographic information system
Corresponding Author:	Silvia Fornasaro, Ph.D. University of Pisa Department of Earth Sciences: Universita degli Studi di Pisa Dipartimento di Scienze della Terra Pisa, Toscana ITALY
First Author:	Silvia Fornasaro, Ph.D.
Order of Authors:	Silvia Fornasaro, Ph.D.
	Guia Morelli
	Valentina Rimondi
	Cesare Fagotti
	Rossella Friani
	Pierfranco Lattanzi
	Pilario Costagliola
Abstract:	In this study, we describe the elaboration of a GIS-based map of the Hg-impacted area of the upper part of the Paglia River basin. The map develops from a systematic collection of all existing geological and geochemical data, together with land cover and geomorphology data, integrated into a GIS-based geo-database. The Hg-impacted area was identified along the upper part of the Paglia River basin and is defined as a band within which there is at least one demonstrated occurrence of sediments/soils with concentrations of Hg ≥1 mg/kg. The Hg-impacted area covers about 20 km2 and the width roughly coincides with the Paglia River floodplain developed in the last 130 years. The identification of a Hg-impacted area will be a useful tool for the local communities in the Paglia River basin and for environmental national agencies when planning works involving the remobilization of sediments to prevent the dispersal of old deposited contaminants. Considering that the extent of the Hg-contaminated area does not allow any remediation, the map can be used for site-specific risk assessment to ensure that anthropogenic activities occur at a minimum risk, considering the opportunity of revising local legislations regarding the permissible Hg-concentration in river/stream sediments in the area.
Suggested Reviewers:	Daniela Zuzolo Università degli Studi del Sannio: Universita degli Studi del Sannio dzuzolo@unisannio.it
	Michal Hosek hosek@iic.cas.cz
	Carmela Rezza carmela.rezza@unina.it

Dear Sirs,

Following a preliminary contact with Dr. Robert Ayuso we attach herewith the manuscript "*A GIS-based map of the Hg-impacted area in the Paglia River basin (Monte Amiata Mining District – Italy): an operational instrument for local authorities*" that we would like to submit for publication in *JGExplo* – special issue on critical elements, edited by Dr. Ayuso and others.

We believe that our paper fits the theme 5 of the special issue. Mercury could have been considered a critical element for most of the 20th century, for its multifold applications. Nowadays it is one of the most feared toxicants – so there is a lesson we could learn on the long-term fate of "critical elements". The Monte Amiata mining district, known since the antiquity and exploited until the 1980s, was the 3rd largest in the world for mercury production. Wastes from mining and smelting are still today major contributors of potentially toxic elements to the aquatic environment. In a sense, this study is a follow up and complement of the paper we recently published in JGExplo (Fornasaro et al., 2022 DOI 10.1016/j.gexplo.2021.106886). In this new paper we have elaborated a GIS-based map of the Hg-impacted area in the Paglia River basin. The map is conceived as a direct operational instrument for the local communities and environmental agencies when planning activities involving the remobilization of sediments, to prevent the dispersal of old deposited contaminants. The paper is complemented by a submission to *Data in brief* of the full dataset used for construction of the map.

We hope that you will find our manuscript suitable for the journal, and we look forward to hearing from you.

Sincerely,

Silvia Fornasaro – on behalf of all co-authors

A GIS-based map of the Hg-impacted area in the Paglia River basin (Monte Amiata Mining District – Italy): an operational instrument for local authorities

S. Fornasaro[1*], G. Morelli[2], V. Rimondi[3], C. Fagotti[4], R. Friani[4], P. Lattanzi[2], P. Costagliola[3]

1 Dipartimento di Scienze della Terra, Università di Pisa, Via Santa Maria, 53, 56126 Pisa, Italy

2 Consiglio Nazionale delle Ricerche (Istituto di Geoscienze e Georisorse), Via G. La Pira, 4, 50121 Firenze, Italy

3 Dipartimento Scienze della Terra, Università di Firenze, Via G. La Pira, 4, 50121 Firenze, Italy

4 Agenzia Regionale per la Protezione dell'Ambiente della Regione Toscana (Area Vasta Sud), Loc. Ruffolo, 53100 Siena, Italy

* silvia.fornasaro@unipi.it

Abstract

In this study, we describe the elaboration of a GIS-based map of the Hg-impacted area of the upper part of the Paglia River basin. The map develops from a systematic collection of all existing geological and geochemical data, together with land cover and geomorphology data, integrated into a GIS-based geo-database. The Hg-impacted area was identified along the upper part of the Paglia River basin and is defined as a band within which there is at least one demonstrated occurrence of sediments/soils with concentrations of Hg ≥1 mg/kg. The Hg-impacted area covers about 20 km^2 and the width roughly coincides with the Paglia River floodplain developed in the last 130 years. The identification of a Hg-impacted area will be a useful tool for the local communities in the Paglia River basin and for environmental national agencies when planning works involving the remobilization of sediments to prevent the dispersal of old deposited contaminants. Considering that the extent of the Hg-contaminated area does not allow any remediation, the map can be used for site-specific risk assessment to ensure that anthropogenic activities occur at a minimum risk, considering the opportunity of revising local legislations regarding the permissible Hg-concentration in river/stream sediments in the area.

Keywords: mercury; Monte Amiata; environmental management; contamination; geographic information system

Highlight

- We elaborate a GIS-based map of a Hg-impacted area in the first segment of the Paglia River basin (Tuscan region)
- The map develops from a systematic collection of all existing geochemical data in the area
- The Hg-impacted area was drawn to include within it all samples having Hg ≥1 mg/kg

- The map intends to be an operational instrument for decision-makers and environmental management

1. Introduction

The Industrial Revolution left a dramatic geochemical imprint in many fluvial systems. Pollution caused by toxic elements employed by the early European industry was so extensive that in many recent stratigraphic fluvial sequences the onset of a polluted layer was proposed as a possible chemical marker for the Anthropocene (Gałuszka et al. 2014). Mercury (Hg) was widely used in the past century by industry (e.g., for industrial chemicals, electrical applications, medical and scientific uses), while at present Hg use and commerce are banned in many countries because of its toxicity, and it is considered a global contaminant (e.g., Chen et al., 2018). Human exposure to Hg mostly occurs by the consumption of medium/large predatory fish, which concentrate Hg due to biomagnification in the food chain. Adverse consequences on human health include neurological and developmental effects that, in turn, have a negative impact even on the gross domestic production (GDP) of large countries like the USA (Spataro et al., 2008).

Contamination of fluvial systems by Hg is reported worldwide, arising from both point and diffuse sources of pollution (e.g., Domagalski, 2001; Gray et al., 2003; Gosar and Teršič 2012; Ebinghaus et al., 2013; Colica et al., 2019; Hošek et al., 2020). Mercury-impacted fluvial systems may represent a transnational issue when the watersheds straddle different countries (e.g., Slovenia and Italy for the Soča/Isonzo River), or eventually affect seaside areas bordering several nations (e.g., Mediterranean Sea). In these environments, Hg may be extremely persistent, and natural attenuation rarely occurs at rates compatible with the human time scale (Fornasaro et al., 2022a). Furthermore, due to the large extension of impacted areas (typically hundreds to thousands of km^2), remediation is in most cases economically unsustainable. Therefore, large Hg masses are constantly reworked in the watersheds (e.g., Rimondi et al., 2019; Fornasaro et al., 2022a), changing spatially with time (Fornasaro et al., 2022a), and eventually being transported to the sea, especially during flood events (Pattelli et al., 2014). Consequently, in many fluvial systems Hg cannot be eliminated, but only controlled. Fluvial valleys and sea basins are natural systems of high and strategic value, where human activities are widespread. The very first step for minimizing the potentially harmful effects of pollutants on these systems is to develop geochemical maps, which define contaminated river corridors adjacent to the impacted waterways. The circumscription of a river corridor, through which contaminated sediments are transported and deposited, contributes to the development of site-specific environmental remediation strategies, to the implementation of monitoring programs and to risk assessment and feasibility study for the involved local authorities.

The Monte Amiata Mining District (MAMD; southern Tuscany, Italy) is known since the Etruscan times (8th century BC) as a source of cinnabar, used as a red pigment. Epithermal-style mineralization postdates the effusive products of the Monte Amiata volcano (ca. 300 ka; Rimondi et al., 2015). Industrial exploitation for mercury production started in the mid-1800s and lasted until the 1980s. Ore smelting and mercury recovery were conducted on site. The total production was at least 102,000 metric tons Hg, making the district the third largest site for Hg production in the world. Indeed, at the beginning of the 20th century, the MAMD contributed to more than 50% of Hg worldwide production (Cipriani & Tanelli, 1983). In this area, mining and smelting played a major role in the dispersal of Hg in the environment. After about 40 years from the end of the extraction works, and despite reclamation of some mining areas (Abbadia San Salvatore and Siele mines), the abandoned mining sites still disperse contaminated water and Hg-rich sediments through the drainage system of the Paglia River (Vaselli et al., 2021; Fornasaro et al., 2022a).

Pollution extends to considerable distances (~200 km from MAMD; Rimondi et al., 2019), crossing three Italian regions (Tuscany, Umbria, and Latium), and eventually reaching the Tiber River, the city of Rome, and the Mediterranean Sea (Fig. 1).

Recent works show that concentrations of Hg downstream the MAMD are above the reference threshold limits for soils for residential/public green land use set by the Italian law (1 mg/kg; D. Lgs. 152/2006) in soil and stream/river sediments along transversal sections of the Paglia River, reaching values of hundreds and, in some cases, thousands of mg/kg (Rimondi et al., 2019; Fornasaro et al., 2022b). In the first segment (~40 km) of the Paglia River, the amount of Hg stored in overbank sediments is estimated to 63 tonnes (Colica et al., 2019) and the contaminated area broadly coincides with the 1954 floodplain (Fornasaro et al., in press). However, the spatial distribution of Hg in the Paglia River floodplain is typically non-uniform (Colica et al., 2019; Rimondi et al., 2019), and contrasting high and low flow conditions and overbank flooding since mining time, contributed to disperse mine contaminated material, making the present floodplain a secondary source of Hg (Colica et al., 2019; Rimondi et al., 2019; Fornasaro et al., 2022b).

The remobilization and redistribution of this mass of Hg contaminated sediments during major flood events presumably will affect the environmental quality of the river and its floodplain for the next future (Pattelli et al., 2014; Colica et al., 2019; Fornasaro et al., 2022b).

In this study, we describe the elaboration of a GIS-based map of the Hg-impacted area in the first segment of the Paglia River basin, from the source to the confluence of the Stridolone Creek, just beyond the Tuscany-Latium regional border (Fig.1), including its main tributaries. The map develops from a systematic collection of all existing geological and geochemical data, together with land cover and geomorphology data, integrated into a GIS-based geo-database (Fornasaro et al., 2022b). The map is intended as a direct operational instrument for

decision-makers, it can be continuously updated and integrated and therefore it is a useful tool for the environmental management of the Paglia River catchment area, where coexistence between humans and Hg contamination should occur at minimum risk. Although restricted to the first segment of the Paglia River basin, the map has obvious implications for the whole Paglia-Tiber River system and the Mediterranean Sea.

2. Study area

The study area (Fig. 1) extends for about 22 km from the Paglia River starting point (the confluence of Pagliola and Cacarello creeks) to the confluence with the Stridolone Creek, covering an area of about 440 km^2, ~48 % of which is occupied by natural features: mainly forests (~35 %) and natural grassland, watercourses, bare rocks (~13 %). The rest (~52 %) is occupied by agricultural (~47 %), industrial (~2.1 %), and residential (~1.6 %) areas, according to the Land Cover Maps of Tuscan and Latium (Regione Toscana, 2019; Regione Lazio, 2000).

The climate of the region is classified as Mediterranean, with mean annual temperatures (1953–2000 period) of 10.5°C. The mean annual precipitations (1925–2000 period) are 1480 mm in 105 rainy days (Ciccacci et al., 2009).

The geology of the area is related to the Tertiary Apennine orogeny and subsequent post-collision events (Brogi, 2008; Molli, 2008; Fig. 1C). These events led to the genesis of extensive magmatic and hydrothermal phenomena, with the development of the Mt. Amiata volcano and the associated geothermal zone (Marroni et al., 2015). As a result of its geodynamic history, the area is characterized by a stack of units over the western edge of the Adria tectonic plate: from bottom to top, these units are composed by i) Tuscan, Ligurian, and Subligurian Units, consisting of fragments of the oceanic basin and its oceanic-continental transition; ii) Neogenic deposits of marine, transition, and continental successions; iii) Quaternary volcanic and volcano-sedimentary successions of Monte Amiata; iv) Holocene fluvial deposits. The latter are present along the Paglia River valley and its main tributaries, consisting mainly of sandy-silty beds and pebbles.

Several abandoned Hg-mines of the MAMD are located on the eastern side of Monte Amiata and are drained by the right-tributaries of the Paglia River: Pagliola, Minestrone, Senna, Siele, and Stridolone creeks (Fig. 1C). The remediation of the mining sites is ongoing at the Abbadia San Salvatore mine (Vaselli et al., 2017), and it was concluded at the Siele mine in 2001 (Fornasaro et al., 2022a).

3. Material and methods

Definition of the "Hg-impacted area"

The definition of the Hg-impacted area, described here also as the “corridor”, is based on the limit set for Hg by the Italian Legislation for soils in residential sites and public green areas, according to which a soil is contaminated if Hg is above 1 mg/kg (D.Lgs. 152/2006).

The corridor (Fig. S1), that extends along the course of the Paglia River as well as its main tributaries (i.e., Pagliola, Minestrone, Senna, Siele and, Stridolone Creeks), was identified by matching the geochemical data (n = 190) collected along transverse sections (transects) along the river as surveyed in previous works (Tab. S1; Fornasaro et al., 2022b, Rimondi et al., 2019, and Colica et al., 2019), with geomorphological features, such as recent fluvial terraces reconstructed by topographic maps and aerial images (Fornasaro et al., 2022b), covering the period of activity of the MAMD. All geochemical and geomorphological data, as well as the recent and old cartography, were plotted in a GIS software to efficiently compare them. Along the transects, the boundaries of the corridor were placed between the last point with Hg ≥1 mg/kg and the first point with Hg <1 mg/kg (limit point) (Fig. 2). Between two transects (i.e., where no geochemical data are available), the limit was drawn up following: 1) from upstream to downstream the contour lines of the altitude of the last limit point of the upstream transect, and gradually connecting it to the height of the limit point of the next transect; 2) the extension limits of impacted recent fluvial terraces, in particular those dating back to 1954, formed during the maximum MAMD activity, that are known to be the most polluted (Colica et al., 2019). Dashed line boundaries indicate sections where available information (geochemical, geomorphological) was limited.

As pointed out by many authors (see Gray et al., 2014 and references therein), Hg analyses of stream sediments or soils impacted by mining/metallurgical activities are affected by the well-known “nugget effect” which may negatively influence the analytical reproducibility. To minimize this effect, in recent sampling surveys (from 2018 onward), each sample was composed of five aliquots picked up from the corners and the center of a square with 2 meters sides. Samples were finely ground and homogenized before analyses (see Fornasaro et al., 2022a for a detailed description of sampling procedure and preparation). However, we noticed that the Hg analytical reproducibility is in general scarce, and differences between different aliquots of the same sample may reach ~50%.

Consequently, in the definition of the corridor, isoconcentration lines/areas were intentionally avoided since the nugget effect makes unreliable any model of a gradual variation of Hg with space. The impacted corridor in the map indicates, therefore, an area where anomalous (≧1 mg/kg) Hg contents were found at least once.

The “Hg-impacted area map” was produced by QGis 3.16 – Hannover on a 1:15.000 scale. The cartographic base is expressed in the WGS84 coordinate reference system to fulfill the ISO standard (i.e., A0 paper size 841 mm-1189 mm, Fig. S1 in *supplementary material*) and, at the same time, to provide a map with good details. The Regional Technical Maps (Carta

tecnica regionale, CTR) of Tuscany and Latium at a 1:10.000 scale (Regione Toscana, 2010; Regione Lazio, 1990) were used as base maps. Adobe Illustrator software was employed to draw and assemble the final map. The Qgis project is included in the supplementary material.

4. Results and discussion

4.1 Impacted area: limits, definition, and implications

The Hg-impacted corridor represents an area where at least one sample of soils and sediments has Hg concentrations ≥1 mg/kg. This criterion does not imply that any other sample collected within the corridor will exceed this value. Similarly, it is possible that new samples collected outside the corridor will display Hg concentration exceeding 1 mg/kg. In this case the corridor limit could be adjusted to include any such sample. The variability of the limits of the impacted corridor are linked to the geological, geomorphological, and geochemical complexity of the area.

In its present form, the impacted corridor covers an area of ~20 km^2, with a variable width, in the order of a few hundreds of meters (Fig. S1), that roughly coincides with the floodplain built by the Paglia River and by its tributaries Siele and Stridolone Creeks in the last 130 years, as identified in Fornasaro et al., 2022b.

The inference made in the map that the area between two transects is impacted by Hg and most probably includes sediments or soils with Hg>1 mg/kg is based on the fact that in the floodplain, river terraces developed by the Paglia River since 1954, the acme of extraction activity in the MAMD, are characterized by a marked and persistent anomaly of Hg (up to 120 mg/kg), as documented by Colica et al. (2019). The temporal and spatial evolution of the floodplain, which led to a distribution of mine waste and contaminated Hg sediments over a vast area (Fornasaro et al., 2022b), contribute to the extension of the impacted corridor.

On the other hand, the Hg-impacted area may locally extend well beyond these geological/geomorphological features. The most evident deviations are recorded near the transects TP1, TP7, and TS1 (Fig. S1), where anomalous values (up to 63 mg/kg; Fornasaro et al., 2022a,b) were found in sediments and soils located at higher altitudes than those reached by the Paglia River and the Siele Creek during recent flood events (e.g., in 2012), and not coincident with the terraces formed in the last 130 years (Fornasaro et al., 2022b). The enlargements of the corridor are observed almost systematically in correspondence with roads, houses, and/or in agricultural facilities of variable size (Fornasaro et al., 2022b). During the mining period the reuse of mine/metallurgical wastes (employed for road embarkments, house foundations, etc.) was a common practice, leading to the suspect that these enlargements are caused by recent anthropic activities. Anomalous Hg concentrations in the area may also be attributed to natural origins (i.e., natural geochemical variability, including the presence of small-scale mineralized bodies). Indeed, the natural Hg background in the

Monte Amiata area, although not precisely established, could be as high as 1-2 mg/kg (Protano and Nannoni, 2018; Rimondi, 2012), and in any case orders of magnitude higher than average crustal values (0.05-0.08 mg/kg; Rudnick et al., 2003), contributing to making the corridor width irregular.

The corridor also includes the final tracts of the main five right-tributaries of the Paglia River draining mining sites (Fig. 1C). The extension of the tracts along the Pagliola Creek was based on transect TP1 and literature data of Rimondi et al. (2014); for the Minestrone and Senna Creek on literature data (RIMIN, 1985; ENEL,1996; Rimondi et al., 2019); for the Siele and Stridolone Creeks, on transects TS1 and TST respectively (Fig. S1).

The fluvial sediments and alluvial soils of the left-tributaries of the Paglia River (i.e., Cacarello, Rigo, Elvella, and Tirolle Creeks) were not included in the impacted area, because they do not drain mines or Hg anomalies. The limit of the corridor along the hydrographic left side of the Paglia River mostly coincides with the Cassia Road pathway (Fig. S1), especially along the tracts where the embankment is close to the river and acts as a bank. However, the fluvial terraces located between the Cassia and the Paglia River are generally high in Hg, either because they were formed during the MAMD activity or because they are easily reached during the floods by Hg-rich sediments eroded upstream (cf., Colica et al., 2019; Pattelli et al., 2014; Fornasaro et al., 2022b).

As highlighted above, the geomorphological and geochemical characteristics of the Paglia River catchment, make it essential to emphasize that the definition of the Hg-impacted area is purely operational and does not necessarily indicate the cause (natural or anthropogenic) of the anomaly itself.

4.2 Soil use and possible practices in the Hg-impacted area

The map highlights that over 83% of the river sediments and soils (n = 190) bordering the river in the upper part of the Paglia River basin have concentrations of Hg higher than 1 mg/kg. Comparison between the land-use map (Regione Toscana, 2019) with the corridor area shows that Hg contamination affects a quite anthropized area (Tab. 1; Fig. 3), as expected in fluvial ecosystems which are providers of important services for local communities (Everard and Quinn, 2015). Based on the current data, remediation of the Paglia fluvial system can be hardly achieved in an economically sustainable way and a correct environmental management of the area is necessary to minimize the risk associated to Hg contamination. In fact, many activities present in the identified corridor, from agriculture, fishing, or land excavation, may be affected by potential environmental issues, highlighting the necessity of further investigation, and monitoring in the area in the future.

For example, i) although studies on speciation in stream sediments in the first tract of the Pagliola Creek pointed out that Hg is mainly bound to insoluble phases (Rimondi et al., 2014),

suggesting that agricultural practices are safe, the presence of some soluble compounds is documented (Rimondi et al., 2014b), and we lack information on the Paglia River tract; ii) along the mapped corridor, Hg methylation was demonstrated in aquatic biota (Rimondi et al., 2012), and a fish ban was adopted by local administrations to prevent the risk to human health; iii) the presence of fluvial quarrying activity for the exploitation of fluvial sediments/terraces along the investigated segment, if not conducted properly, can significantly influence the mobility of Hg and its transport through the river system, and finally to the Mediterranean Sea. These quarries generally select coarse sediments from sand fraction upwards. The fine fraction with no commercial value is usually stored into artificial basins near the river course; this fine fraction (<250 μm) of soil and sediments along the Paglia River contains almost all the Hg of the total sample (Colica et al., 2019). Furthermore, iv) any new industrial settlement in the area will involve the mobilization of potentially Hg-contaminated material, with its associated environmental risks. For instance, a project for the construction of a new geothermal power plant in the alluvial plain between transects TP1 and TP2 has recently been approved. In general, v) any earthmoving caused by anthropogenic factors within the impacted area is potentially able to mobilize sediments downstream with high Hg concentrations. Large excavation works, carried out in winter 2020 along a section of few hundred meters in the Paglia riverbed to restore a tract of the Cassia Road, collapsed in consequence of a flood event, and produced the mobilization of sediments and turbid clouds along the river.

Moreover, comparison with the hydraulic hazard map (Piano Stralcio di Assetto Idrogeologico, 2006) shows that along the Paglia River the area corresponding to the high hydraulic hazard, with a return time of 50 years (P3 area in the Piano Stralcio di Assetto Idrogeologico, 2006) falls within the Hg-impacted area (Fig. 4). This suggests that during flood events, there is the risk that contaminated soils or sediments in the impacted area can be eroded and transported downstream. Part of these sediments may be redeposited on recent overbank terraces, as documented by Pattelli et al. (2014) during the 2012 flood of the Paglia River, but ultimately their final destination is the Mediterranean Sea. The implications of Hg distribution in the Paglia River catchment go beyond the local impact, highlighting the opportunity of tracing the impacted corridor beyond the regional border, and eventually of estimating its consequences on a transnational (Mediterranean) scale.

Indeed, this study provide useful information for management authorities to identify conservation measures in this area (e.g., tree planting on overbanks, retention basins, thresholds and/or selective weirs; see Allen et al., 2016).

The most likely source of Hg in the river courses of the Paglia basin derives from past mining and smelting activities occurred in the Monte Amiata district. The reclamation works at the mining sites that were carried out, or are in progress, or will occur in the future, will hopefully

minimize the input of new contaminated material, but will not stop the redistribution of what has been deposited in the river system presumably for decades.

Therefore, the resulting map of the spatial distribution of Hg contamination along the Paglia River associated to the knowledge of the factors determining its extension (Fornasaro et al., 2022b) will contribute to assess the specific risk posed by Hg and to develop site specific legislations for the anthropic practices that may or may not be conducted along the identified corridor.

Another important use of the map will be its utility in dissemination projects (e.g., LIFE projects of the EU) aimed at spreading knowledge of the contamination problem to the population and creating awareness of the possible coexistence between humans and heavy metals in Tuscany as elsewhere. A limitation of the current map is the lack of the third dimension. Drilling surveys with a total recovery of the drill core are planned to estimate the depth reached by the Hg anomaly.

5. Conclusions

Based on collation of all available data, a Hg-impacted area was identified along the upper part of the Paglia River basin (Tuscan region), defined as a band within which there is at least one demonstrated occurrence of sediments/soils with concentrations of Hg ≥1 mg/kg. The Hg-impacted area covers about 20 km^2, and its width roughly coincides with the floodplain of the Paglia River and its tributaries (i.e., Siele and Stridolone creeks) as developed in the last 130 years (Fornasaro et al., 2022b). The resulting map shows that the Hg-impacted area along the Paglia River is almost entirely within the area at risk of floods. The environmental problem caused by the presence of Hg in the corridor has effects not only on local practices (agriculture, fishing, etc.), but also at regional or transnational scale. The Hg-impacted area map represents an essential operational instrument for the local communities for a correct environmental management of the area to minimize the risks associated to works involving the remobilization of sediments (e.g., quarries, modification of riverbanks, excavations for agricultural or industrial activities), as well as to prevent Hg exposure pathways to humans. The existence of industrial activities and residential areas located within the contaminated corridor suggests the opportunity of revising the current legislation regarding the permissible concentration of Hg in river/stream sediments, considering also that the extent of the identified Hg-contaminated area does not allow any permanent environmental remediation.

Also, the environmental database developed in this study can be regarded as a first step for the establishment of a web-based GIS Decision Support System for the regional environmental protection agencies (ARPA) and local authorities. This system is expected to make environmental data available through the web to support decision-makers in implementing a reclamation program for the abandoned MAMD site, or in understanding and

forecasting how mine pollution can affect the surrounding ecosystems, and it will overcome the existing difficulties in combining numerous spatial-related parameters in environmental studies. The map and the linked database are easily mineable and, hence, in collaboration with the regional authority, the map could be uploaded to the website of regional environmental agencies. Finally, the elaborated geo-database scheme can be applied in any other abandoned mining site to assess the extent of environmental contamination.

Silvia Fornasaro: Investigation, Data curation, Writing – Original Draft, Writing - Review & Editing. **Guia Morelli**: Investigation, Data curation, Writing - Review & Editing. **Valentina Rimondi**: Investigation, Data curation, Writing - Review & Editing. **Cesare Fagotti**: Funding acquisition, Supervision, Investigation, Writing - Review & Editing. **Rossella Friani**: Methodology, Writing - Review & Editing. **Pierfranco Lattanzi**: Investigation, Data curation, Writing – Original Draft, Writing - Review & Editing. **Pilario Costagliola**: Funding acquisition, Supervision, Investigation, Data curation, Writing – Review & Editing.

References

Allen, D. C., Cardinale, B. J., & Wynn-Thompson, T. (2016). Plant biodiversity effects in reducing fluvial erosion are limited to low species richness. Ecology, 97(1), 17-24.

Brogi, A. (2008). The structure of the Monte Amiata volcano-geothermal area (Northern Apennines, Italy): Neogene-Quaternary compression versus extension. International Journal of Earth Sciences, 97(4), 677-703.

Chen, C. Y., Driscoll, C. T., Eagles-Smith, C. A., Eckley, C. S., Gay, D. A., Hsu-Kim, H., & Thompson, M. R. (2018). A critical time for mercury science to inform global policy.

Ciccacci, S., Galiano, M., Roma, M. A., & Salvatore, M. C. (2009). Morphodynamics and morphological changes of the last 50 years in a badland sample area of Southern Tuscany (Italy). Zeitschrift fur Geomorphologie, 53(3), 273.

Cipriani C., Tanelli G. Risorse minerarie ed industria estrattiva in Toscana. Note storiche ed economiche Atti e Memorie Accademia di Scienze e Lettere La Colombaria, 28 (1983), pp. 241-283 (in Italian)

Colica, A., Benvenuti, M., Chiarantini, L., Costagliola, P., Lattanzi, P., Rimondi, V., & Rinaldi, M. (2019). From point source to diffuse source of contaminants: The example of mercury dispersion in the Paglia River (Central Italy). Catena, 172, 488-500.

Cosentino D. & Pasquali V. (2012) - Carta Geologica Informatizzata della Regione Lazio. Università degli Studi Roma Tre - Dipartimento di Scienze Geologiche, Regione Lazio - Agenzia Regionale Parchi Area Difesa del Suolo; http://dati.lazio.it/catalog/it/dataset/cartageologica-informatizzata-regione- lazio-25000.

D.Lgs. (2006). Decreto Legislativo 3 aprile 2006, n. 152-Norme in materia ambientale.

Domagalski, J. (2001). Mercury and methylmercury in water and sediment of the Sacramento River Basin, California. Applied Geochemistry, 16(15), 1677-1691.

Ebinghaus, R., Turner, R. R., de Lacerda, L. D., Vasiliev, O., & Salomons, W. (Eds.). (2013). Mercury contaminated sites: characterization, risk assessment and remediation. Springer Science & Business Media.

ENEL, 1996. Indagine per la valutazione degli effetti sull'ambiente delle emissioni aerodisperse degli impianti geotermoelettrici dell'area amiatina. Relazione generale. Roma (in Italian)

Everard, M., & Quinn, N. (2015). Realizing the value of fluvial geomorphology. International Journal of River Basin Management, 13(4), 487-500.

Fornasaro, S., Morelli, G., Rimondi, V., Fagotti, C., Friani, R., Lattanzi, P., & Costagliola, P. (2022). Mercury distribution around the Siele Hg mine (Mt. Amiata district, Italy) twenty years after reclamation: Spatial and temporal variability in soil, stream sediments, and air. Journal of Geochemical Exploration, https://doi.org/10.1016/j.gexplo.2021.106886

Fornasaro, S., Morelli, G., Rimondi, V., Fagotti, C., Friani, R., Lattanzi, P., & Costagliola, P. (2022). The extensive mercury contamination in soil and legacy sediments of the Paglia River basin (Tuscany, Italy): interplay between Hg-mining waste discharge along rivers, 1960s economic boom, and ongoing climate change. Journal of Soils and Sediments, 1-16. https://doi.org/10.1007/s11368-021-03129-0

Fornasaro S., Morelli G., Rimondi V., Fagotti C., Lattanzi P., Costagliola P. (b) Mercury and Methylmercury dataset from soil, sediments, air, mine-waste, and water in the Paglia River basin (Monte Amiata Mining District – Central Italy). Data in Brief, under review.

Gałuszka, A., Migaszewski, Z. M., & Zalasiewicz, J. (2014). Assessing the Anthropocene with geochemical methods. Geological Society, London, Special Publications, 395(1), 221-238.

Gosar, M., & Teršič, T. (2012). Environmental geochemistry studies in the area of Idrija mercury mine, Slovenia. Environmental geochemistry and health, 34(1), 27-41.

Gray, J. E., Greaves, I. A., Bustos, D. M., & Krabbenhoft, D. P. (2003). Mercury and methylmercury contents in mine-waste calcine, water, and sediment collected from the Palawan Quicksilver Mine, Philippines. Environmental Geology, 43(3), 298-307.

Gray, J. E., Rimondi, V., Costagliola, P., Vaselli, O., & Lattanzi, P. (2014). Long-distance transport of Hg, Sb, and As from a mined area, conversion of Hg to methyl-Hg, and uptake of Hg by fish on the Tiber River basin, west-central Italy. Environmental geochemistry and health, 36(1), 145-157.

Hošek, M., Bednárek, J., Popelka, J., Elznicová, J., Tůmová, Š., Rohovec, J. & Grygar, T. M. (2020). Persistent mercury hot spot in Central Europe and Skalka Dam reservoir as a long-term mercury trap. Environmental geochemistry and health, 42(5), 1273-1290.

Marroni, M., Moratti, G., Costantini, A., Conticelli, S., Benvenuti, M. G., Pandolfi, L., & Laurenzi, M. A. (2015). Geology of the Monte Amiata region, southern Tuscany, central Italy. Italian Journal of Geosciences, 134(2), 171-199.

Molli, G. (2008). Northern Apennine–Corsica orogenic system: an updated overview. Geological Society, London, Special Publications, 298(1), 413-442.

Pattelli, G., Rimondi, V., Benvenuti, M., Chiarantini, L., Colica, A., Costagliola, P., & Rinaldi, M. (2014). Effects of the November 2012 flood event on the mobilization of Hg from the Mount Amiata Mining District to the sediments of the Paglia River Basin. Minerals, 4(2), 241-256.

Piano di Assetto Idrogeologico, Autorità di bacino del fiume Tevere, Roma, 2006

Protano, G., & Nannoni, F. (2018). Influence of ore processing activity on Hg, As and Sb contamination and fractionation in soils in a former mining site of Monte Amiata ore district (Italy). Chemosphere, 199, 320-330.

REGIONE LAZIO (1990) – Carta Tecnica regionale della Regione Lazio alla scala 1:10.000, Roma

Regione Lazio, 2000 Carta dell'uso del suolo. Assessorato urbanistica e casa – Regione Lazio. Scala 1:25,000 Regione Lazio, Roma, Italy (2000)

Regione Toscana, 2010. Carta Tecnica Regionale 1:10000 numerica livello 3 (Regional Technical Map 1.10000 numerical format, level 3). Servizio Cartografico della Regione Toscana, Florence, Italy, 48pp

Regione Toscana, 2018. Carta geologica regionale, scale 1:10.000. http://www502.regione.toscana.it/geoscopio/geologia.html

Regione Toscana, 2019. Carta dell'uso del suolo, scale 1:10.000. http://www502.regione.toscana.it/geoscopio/usocoperturasuolo.html

RIMIN S.P.A. – ENI (1985) – Toscana 2-2bis. Relazione conclusiva sui lavori svolti nell'ambito della convenzione con il Ministero dell'Industria, del commercio e dell'Artigianato. Direzione Generale Miniere.

Rimondi, V. (2012). Distribution of mercury and other trace elements in the Mt. Amiata region (Southern Tuscany, Italy) (Doctoral dissertation, PhD dissertation. Firenze University, Firenze).

Rimondi, V., Chiarantini, L., Lattanzi, P., Benvenuti, M., Beutel, M., Colica, A. & Ruggieri, G. (2015). Metallogeny, exploitation and environmental impact of the Mt. Amiata mercury ore district (Southern Tuscany, Italy). Italian Journal of Geosciences, 134(2), 323-336.

Rimondi, V., Costagliola, P., Gray, J. E., Lattanzi, P., Nannucci, M., Paolieri, M., & Salvadori, A. (2014). Mass loads of dissolved and particulate mercury and other trace elements in the Mt. Amiata mining district, Southern Tuscany (Italy). Environmental Science and Pollution Research, 21(8), 5575-5585.

Rimondi, V., Costagliola, P., Lattanzi, P., Morelli, G., Cara, G., Cencetti, C. & Torricelli, S. (2019). A 200 km-long mercury contamination of the Paglia and Tiber floodplain: Monitoring results and implications for environmental management. Environmental Pollution, 255, 113191.

Rudnick, R. L., Gao, S., Holland, H. D., & Turekian, K. K. (2003). Composition of the continental crust. The crust, 3, 1-64.

Vaselli, O., Lazzaroni, M., Nisi, B., Cabassi, J., Tassi, F., Rappuoli, D., & Meloni, F. (2021). Discontinuous Geochemical Monitoring of the Galleria Italia Circumneutral Waters (Former Hg-Mining Area of Abbadia San Salvatore, Tuscany, Central Italy) Feeding the Fosso Della Chiusa Creek. Environments, 8(2), 15.

Vaselli, O., Nisi, B., Rappuoli, D., Cabassi, J., & Tassi, F. (2017). Gaseous elemental mercury and total and leached mercury in building materials from the former Hg-mining area of Abbadia San Salvatore (Central Italy). International journal of environmental research and public health, 14(4), 42.

Figures

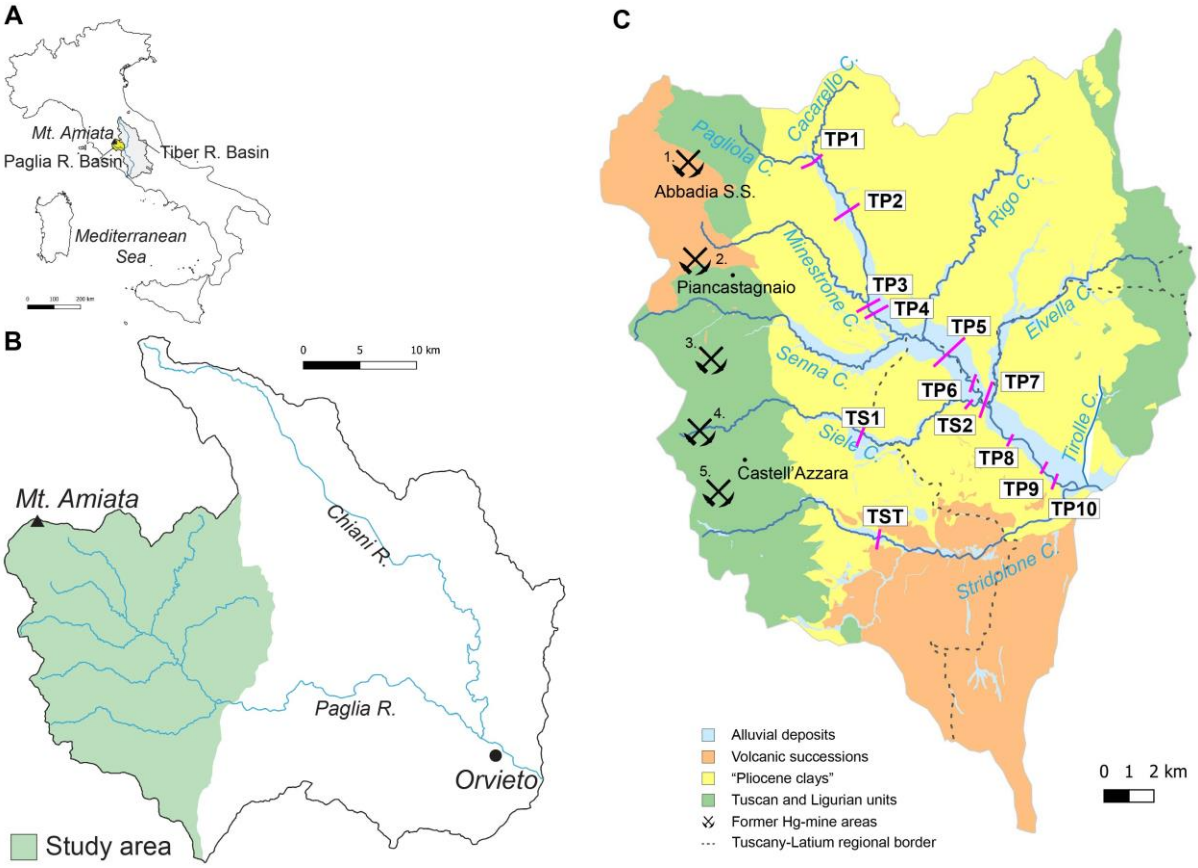

Fig. 1 Location of (A) the Paglia-Tiber River system and (B) the study area; (C) geological map with location of the sampling transects and of the main mining areas: 1) Abbadia San Salvatore; 2) Case di Paolo; 3) Senna; 4) Siele; 5) Cornacchino.

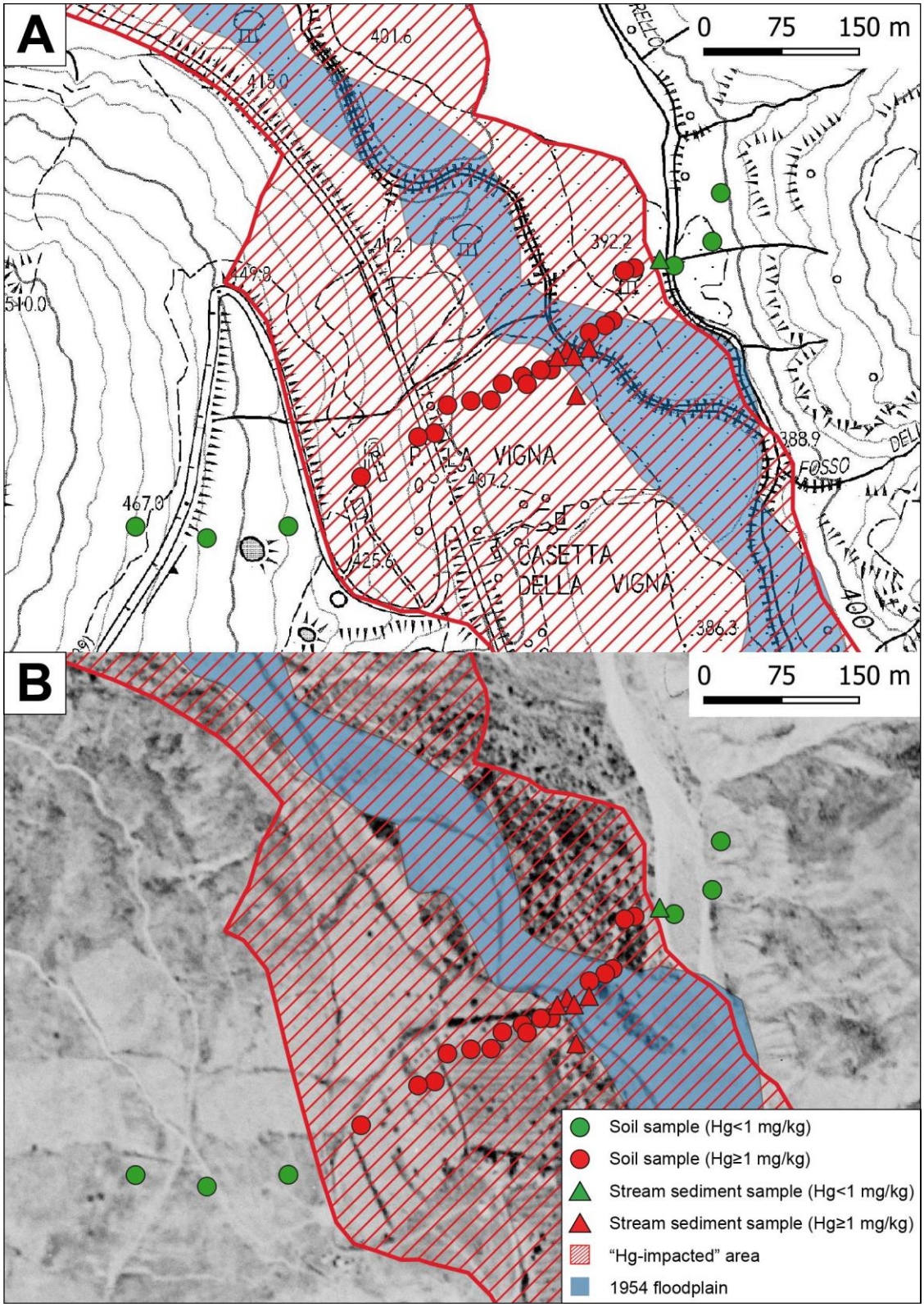

Fig. 2 Criteria followed to define the Hg-impacted area: example along one of the transects in the Paglia River: a) topographic map; b) floodplain in 1954.

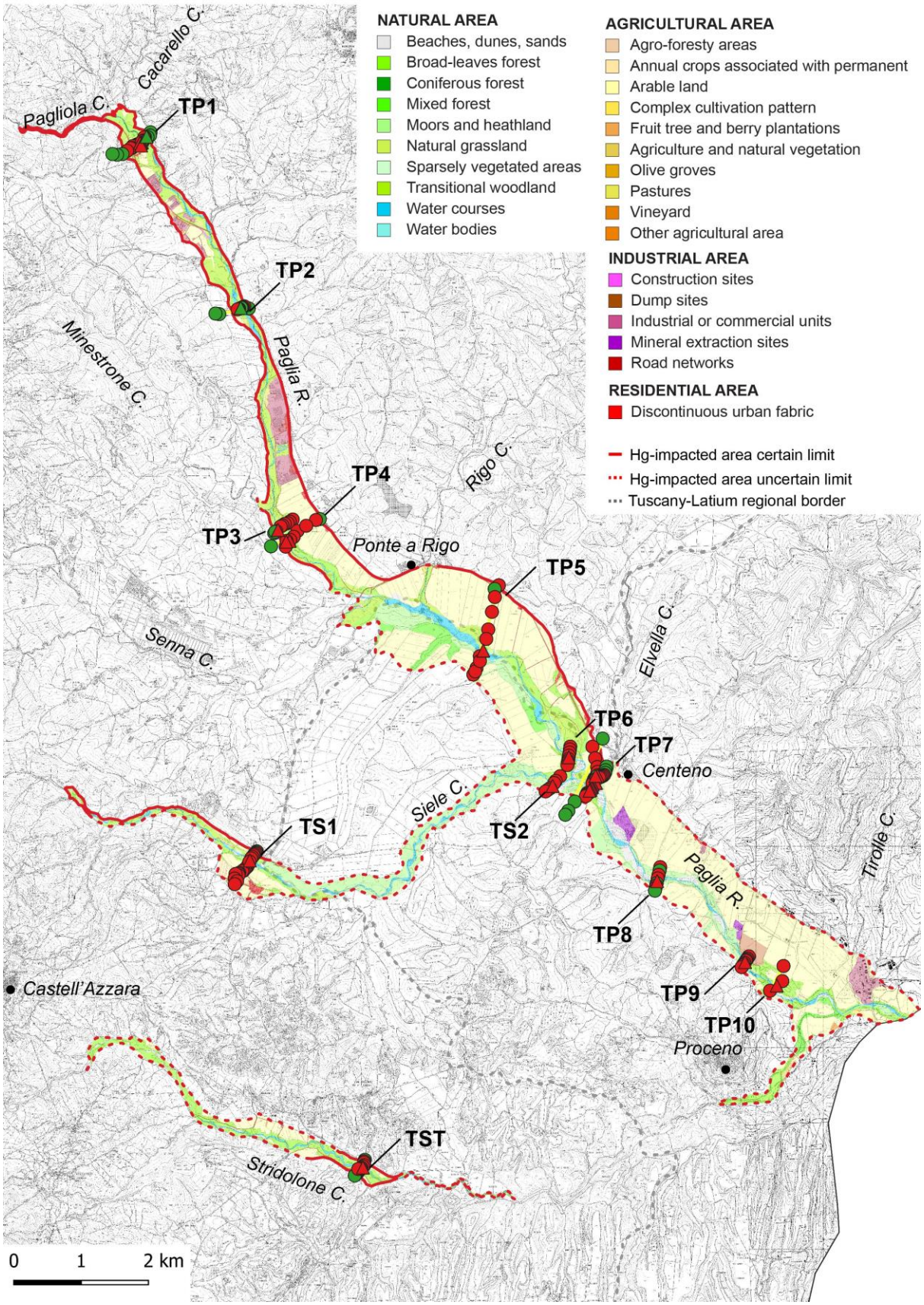

Fig. 3 Land use (Regione Toscana, 2019; Regione Lazio, 2000) within the Hg-impacted area. The location of the sampling transects is also reported.

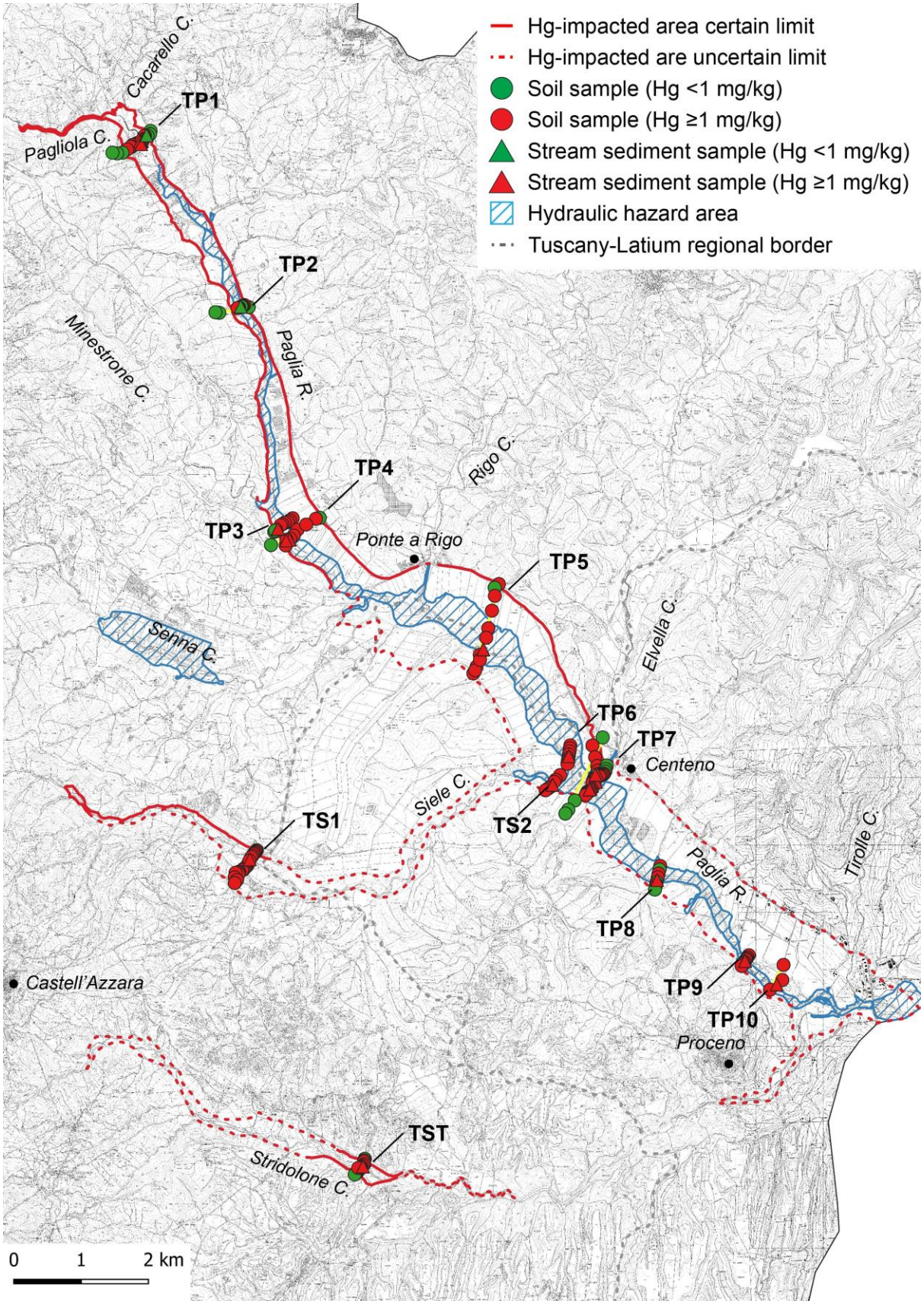

Fig. 4 Map of the Hg-impacted area compared to the hydraulic hazard map (Piano Stralcio di Assetto Idrogeologico, 2006). *The location of the sampling transects is also reported.*

Fig. S1 The GIS-based map of the Hg-impacted area in the Paglia River basin (Monte Amiata Mining District – Italy), with the location of the sampling transects. Alluvial deposits were reported from the geological maps of Cosentino and Pasquali (2012) and Regione Toscana (2018).

Tables

Tables

IMPACTED AREA		Area			
Use-Area	**Use-Class**	**km²**	**%**	**km²**	**%**
Agricultural area	Agro-forestry areas	0.003	0.01	**9.37**	**51.15**
	Annual crops associated with permanent	0.05	0.28		
	Arable land	9.06	49.47		
	Complex cultivation	0.03	0.15		
	Fruit trees and berry plantations	0.01	0.07		
	Land principally occupied by agriculture, with significant areas of natural vegetation	0.02	0.11		
	Olive groves	0.02	0.13		
	Other agricultural area	0.12	0.67		
	Pastures	0.02	0.11		
	Vineyards	0.03	0.14		
Industrial area	Construction sites	0.01	0.03	**1.00**	**5.49**
	Dump sites	0.01	0.05		
	Industrial or commercial units	0.62	3.40		
	Mineral extraction sites	0.10	0.57		
	Road and rail networks and associated land	0.26	1.44		
Natural area	Beaches, dunes, and sand plains	0.41	2.22	**7.87**	**42.99**
	Broad-leaved forest	2.13	11.65		
	Coniferous forest	0.07	0.39		
	Mixed forest	0.42	2.27		
	Moors and heathland	2.05	11.20		
	Natural grassland	0.05	0.29		
	Sparsely vegetated areas	0.00	0.01		
	Transitional woodland shrub	1.76	9.61		
	Water bodies	0.01	0.06		
	Water courses	0.97	5.29		
Residential area	Discontinuous urban fabric	0.07	0.38	**0.07**	**0.38**
Total		*18.31*	*100*	*18.31*	*100*

Tab. 1 Land use in the identified Hg-impacted area. Land use data are from Regione Toscana, 2019

Id	Transect	Matrix	Lat	Lon	Hgt (mg/kg)	Reference
TP1_17	**TP1**	Stream sediment	42.88280	11.72850	34	Fornasaro et al., 2022b
TP1_19	**TP1**	Soil	42.88291	11.72792	43	Fornasaro et al., 2022b
TP1_27	**TP1**	Soil	42.88174	11.72504	<0.2	Fornasaro et al., 2022b
TP1_28	**TP1**	Soil	42.88166	11.72407	0.27	Fornasaro et al., 2022b
TP1_29	**TP1**	Soil	42.88178	11.72323	<0.2	Fornasaro et al., 2022b

TP1_1	**TP1**	Soil	42.88452	11.73029	<0.2	Rimondi et al., 2019
TP1_10	**TP1**	Stream sediment	42.88321	11.72867	64	Rimondi et al., 2019
TP1_11	**TP1**	Stream sediment	42.88320	11.72841	28	Rimondi et al., 2019
TP1_12	**TP1**	Stream sediment	42.88314	11.72849	37	Rimondi et al., 2019
TP1_13	**TP1**	Stream sediment	42.88314	11.72829	12.7	Rimondi et al., 2019
TP1_14	**TP1**	Soil	42.88303	11.72821	0.99	Rimondi et al., 2019
TP1_15	**TP1**	Soil	42.88303	11.72821	3	Rimondi et al., 2019
TP1_16	**TP1**	Soil	42.88303	11.72809	42	Rimondi et al., 2019
TP1_18	**TP1**	Soil	42.88298	11.72787	34	Rimondi et al., 2019
TP1_2	**TP1**	Soil	42.88410	11.73017	<0.2	Rimondi et al., 2019
TP1_20	**TP1**	Soil	42.88292	11.72763	7.4	Rimondi et al., 2019
TP1_21	**TP1**	Soil	42.88278	11.72749	8.3	Rimondi et al., 2019
TP1_22	**TP1**	Soil	42.88278	11.72725	16.7	Rimondi et al., 2019
TP1_23	**TP1**	Soil	42.88275	11.72697	1.75	Rimondi et al., 2019
TP1_24	**TP1**	Soil	42.88251	11.72681	21	Rimondi et al., 2019
TP1_25	**TP1**	Soil	42.88248	11.72661	3.4	Rimondi et al., 2019
TP1_26	**TP1**	Soil	42.88215	11.72592	12	Rimondi et al., 2019
TP1_3	**TP1**	Soil	42.88390	11.72971	<0.2	Rimondi et al., 2019
TP1_4	**TP1**	Stream sediment	42.88396	11.72954	<0.2	Rimondi et al., 2019
TP1_5	**TP1**	Soil	42.88389	11.72924	33	Rimondi et al., 2019
TP1_6	**TP1**	Soil	42.88387	11.72912	100	Rimondi et al., 2019
TP1_7	**TP1**	Soil	42.88344	11.72896	93	Rimondi et al., 2019
TP1_8	**TP1**	Soil	42.88340	11.72887	21	Rimondi et al., 2019
TP1_9	**TP1**	Soil	42.88334	11.72868	32	Rimondi et al., 2019
TP10_1	**TP10**	Soil	42.77014	11.84029	8.9	Rimondi et al., 2019
TP10_2	**TP10**	Soil	42.76812	11.83998	11	Rimondi et al., 2019
TP10_3	**TP10**	Stream sediment	42.76755	11.83895	8.9	Rimondi et al., 2019
TP10_4	**TP10**	Soil	42.76690	11.83769	11	Rimondi et al., 2019
TP2_2	**TP2**	Soil	42.86082	11.74630	66.9	Colica et al., 2019
TP2_3	**TP2**	Soil	42.86074	11.74604	13	Colica et al., 2019
TP2_4	**TP2**	Soil	42.86068	11.74588	97	Colica et al., 2019
TP2_5	**TP2**	Soil	42.86065	11.74577	0.6	Colica et al., 2019
TP2_6	**TP2**	Stream sediment	42.86062	11.74565	0.2	Colica et al., 2019
TP2_7	**TP2**	Soil	42.86052	11.74534	4.3	Colica et al., 2019
TP2_8	**TP2**	Soil	42.86049	11.74522	1.3	Colica et al., 2019
TP2_9	**TP2**	Soil	42.86044	11.74506	8.3	Colica et al., 2019
TP2_1	**TP2**	Soil	42.86052	11.74710	<0.2	Fornasaro et al., 2022b
TP2_10	**TP2**	Soil	42.85989	11.74170	0.39	Fornasaro et al., 2022b
TP2_11	**TP2**	Soil	42.85998	11.74102	<0.2	Fornasaro et al., 2022b
TP3_10	**TP3**	Soil	42.83034	11.75040	0.2	Colica et al., 2019
TP3_10	**TP3**	Soil	42.83208	11.75384	3.5	Colica et al., 2019
TP3_2	**TP3**	Soil	42.83181	11.75329	2.9	Colica et al., 2019

TP3_3	**TP3**	Soil	42.83161	11.75291	5.9	Colica et al., 2019
TP3_4	**TP3**	Soil	42.83152	11.75236	40	Colica et al., 2019
TP3_5	**TP3**	Soil	42.83133	11.75193	40.3	Colica et al., 2019
TP3_6	**TP3**	Soil	42.83120	11.75161	10.9	Colica et al., 2019
TP3_7	**TP3**	Stream sediment	42.83075	11.75110	3.5	Colica et al., 2019
TP3_8	**TP3**	Soil	42.83057	11.75079	17.3	Colica et al., 2019
TP3_9	**TP3**	Soil	42.83050	11.75059	0.1	Colica et al., 2019
TP4_1	**TP4**	Soil	42.83202	11.75876	0.8	Fornasaro et al., 2022b
TP4_10	**TP4**	Soil	42.82848	11.75239	6.6	Fornasaro et al., 2022b
TP4_11	**TP4**	Soil	42.82859	11.74974	<0.2	Fornasaro et al., 2022b
TP4_2	**TP4**	Soil	42.83191	11.75806	17.3	Fornasaro et al., 2022b
TP4_4	**TP4**	Soil	42.83052	11.75463	2	Fornasaro et al., 2022b
TP4_4	**TP4**	Soil	42.83118	11.75625	5.9	Fornasaro et al., 2022b
TP4_5	**TP4**	Soil	42.82975	11.75390	1.2	Fornasaro et al., 2022b
TP4_6	**TP4**	Soil	42.82936	11.75326	75	Fornasaro et al., 2022b
TP4_7	**TP4**	Stream sediment	42.82922	11.75316	28	Fornasaro et al., 2022b
TP4_8	**TP4**	Soil	42.82924	11.75259	17	Fornasaro et al., 2022b
TP4_9	**TP4**	Stream sediment	42.82914	11.75251	47	Fornasaro et al., 2022b
TP5_10	**TP5**	Soil	42.81141	11.78636	16.8	Colica et al., 2019
TP5_3	**TP5**	Soil	42.82081	11.79011	22.6	Colica et al., 2019
TP5_4	**TP5**	Soil	42.81884	11.78949	4.4	Colica et al., 2019
TP5_5	**TP5**	Soil	42.81650	11.78871	2.6	Colica et al., 2019
TP5_6	**TP5**	Soil	42.81524	11.78829	5	Colica et al., 2019
TP5_7	**TP5**	Stream sediment	42.81370	11.78767	4.1	Colica et al., 2019
TP5_8	**TP5**	Soil	42.81297	11.78702	6	Colica et al., 2019
TP5_9	**TP5**	Soil	42.81231	11.78701	12.3	Colica et al., 2019
TP5_1	**TP5**	Soil	42.82237	11.79091	5.1	Fornasaro et al., 2022b
TP5_11	**TP5**	Soil	42.81053	11.78573	2.8	Fornasaro et al., 2022b
TP5_12	**TP5**	Soil	42.81094	11.78610	2.6	Fornasaro et al., 2022b
TP5_2	**TP5**	Soil	42.82189	11.79012	<0.2	Fornasaro et al., 2022b
TP6_1	**TP6**	Soil	42.80046	11.80291	49	Colica et al., 2019
TP6_2	**TP6**	Soil	42.80008	11.80282	45.2	Colica et al., 2019
TP6_3	**TP6**	Soil	42.79967	11.80274	5.6	Colica et al., 2019
TP6_4	**TP6**	Soil	42.79925	11.80259	2.5	Colica et al., 2019
TP6_5	**TP6**	Stream sediment	42.79903	11.80257	3.3	Colica et al., 2019
TP6_6	**TP6**	Soil	42.79880	11.80249	4.3	Colica et al., 2019
TP6_7	**TP6**	Soil	42.79854	11.80241	6.2	Colica et al., 2019
TP6_8	**TP6**	Soil	42.79831	11.80236	6.3	Colica et al., 2019
TP6_9	**TP6**	Soil	42.79800	11.80227	7.2	Colica et al., 2019
TP7_1	**TP7**	Soil	42.80139	11.80884	0.2	Fornasaro et al., 2022b
TP7_14	**TP7**	Stream sediment	42.79548	11.80736	9.6	Fornasaro et al., 2022b
TP7_2	**TP7**	Soil	42.80035	11.80693	2.3	Fornasaro et al., 2022b
TP7_29	**TP7**	Soil	42.79308	11.80339	<0.2	Fornasaro et al., 2022b

TP7_3	**TP7**	Soil	42.79879	11.80734	9.2	Fornasaro et al., 2022b
TP7_30	**TP7**	Soil	42.79187	11.80216	<0.2	Fornasaro et al., 2022b
TP7_31	**TP7**	Soil	42.79136	11.80160	<0.2	Fornasaro et al., 2022b
TP7_4	**TP7**	Soil	42.79760	11.80767	10	Fornasaro et al., 2022b
TP7_5	**TP7**	Soil	42.79695	11.80770	1.3	Fornasaro et al., 2022b
TP7_6	**TP7**	Soil	42.79649	11.80769	0.44	Fornasaro et al., 2022b
TP7_7	**TP7**	Soil	42.79649	11.80769	0.45	Fornasaro et al., 2022b
TP7_8	**TP7**	Stream sediment	42.79649	11.80769	1.7	Fornasaro et al., 2022b
TP7_9	**TP7**	Stream sediment	42.79642	11.80730	6.7	Fornasaro et al., 2022b
TP7_10	**TP7**	Soil	42.79620	11.80722	3	Rimondi et al., 2019
TP7_11	**TP7**	Soil	42.79602	11.80705	2.7	Rimondi et al., 2019
TP7_12	**TP7**	Soil	42.79588	11.80697	15	Rimondi et al., 2019
TP7_13	**TP7**	Soil	42.79572	11.80688	22	Rimondi et al., 2019
TP7_15	**TP7**	Soil	42.79553	11.80675	1.5	Rimondi et al., 2019
TP7_16	**TP7**	Soil	42.79540	11.80672	14.85	Rimondi et al., 2019
TP7_17	**TP7**	Stream sediment	42.79528	11.80672	2.6	Rimondi et al., 2019
TP7_18	**TP7**	Stream sediment	42.79500	11.80660	19.7	Rimondi et al., 2019
TP7_19	**TP7**	Stream sediment	42.79488	11.80645	15.8	Rimondi et al., 2019
TP7_2	**TP7**	Soil	42.79739	11.80930	0.39	Rimondi et al., 2019
TP7_20	**TP7**	Stream sediment	42.79460	11.80630	28	Rimondi et al., 2019
TP7_21	**TP7**	Stream sediment	42.79448	11.80613	18.6	Rimondi et al., 2019
TP7_22	**TP7**	Soil	42.79422	11.80605	100	Rimondi et al., 2019
TP7_23	**TP7**	Soil	42.79418	11.80602	21	Rimondi et al., 2019
TP7_24	**TP7**	Soil	42.79424	11.80589	53	Rimondi et al., 2019
TP7_25	**TP7**	Soil	42.79416	11.80569	96	Rimondi et al., 2019
TP7_26	**TP7**	Soil	42.79401	11.80559	79	Rimondi et al., 2019
TP7_27	**TP7**	Soil	42.79387	11.80550	67	Rimondi et al., 2019
TP7_28	**TP7**	Soil	42.79377	11.80543	48	Rimondi et al., 2019
TP7_E1	**TP7**	Soil	42.79762	11.80938	<0.2	Rimondi et al., 2019
TP7_E10	**TP7**	Soil	42.79610	11.80771	4.3	Rimondi et al., 2019
TP7_E11	**TP7**	Soil	42.79603	11.80746	2.8	Rimondi et al., 2019
TP7_E3	**TP7**	Soil	42.79714	11.80918	<0.2	Rimondi et al., 2019
TP7_E4	**TP7**	Soil	42.79680	11.80908	0.56	Rimondi et al., 2019
TP7_E5	**TP7**	Soil	42.79652	11.80887	2.4	Rimondi et al., 2019
TP7_E6	**TP7**	Soil	42.79641	11.80871	1.33	Rimondi et al., 2019
TP7_E7	**TP7**	Soil	42.79633	11.80846	2.7	Rimondi et al., 2019
TP7_E8	**TP7**	Soil	42.79625	11.80821	1.43	Rimondi et al., 2019
TP7_E9	**TP7**	Soil	42.79618	11.80796	3.2	Rimondi et al., 2019
TP8_1	**TP8**	Soil	42.78393	11.81851	3.3	Colica et al., 2019
TP8_2	**TP8**	Soil	42.78346	11.81837	0.4	Colica et al., 2019
TP8_3	**TP8**	Soil	42.78291	11.81816	24.5	Colica et al., 2019

TP8_4	**TP8**	Soil	42.78243	11.81799	22.4	Colica et al., 2019
TP8_5	**TP8**	Stream sediment	42.78207	11.81786	27.5	Colica et al., 2019
TP8_6	**TP8**	Soil	42.78179	11.81777	0.4	Colica et al., 2019
TP8_7	**TP8**	Soil	42.78150	11.81766	6.4	Colica et al., 2019
TP8_8	**TP8**	Soil	42.78116	11.81753	33.2	Colica et al., 2019
TP8_9	**TP8**	Soil	42.78080	11.81741	0.7	Colica et al., 2019
TP9_1	**TP9**	Soil	42.77159	11.83405	1.1	Colica et al., 2019
TP9_2	**TP9**	Soil	42.77131	11.83377	21.4	Colica et al., 2019
TP9_3	**TP9**	Soil	42.77114	11.83361	17.9	Colica et al., 2019
TP9_4	**TP9**	Soil	42.77101	11.83349	15.4	Colica et al., 2019
TP9_5	**TP9**	Stream sediment	42.77084	11.83333	25.1	Colica et al., 2019
TP9_6	**TP9**	Soil	42.77074	11.83323	5.5	Colica et al., 2019
TP9_7	**TP9**	Soil	42.77057	11.83305	15.6	Colica et al., 2019
TP9_8	**TP9**	Soil	42.77040	11.83289	53.6	Colica et al., 2019
TP9_9	**TP9**	Soil	42.77018	11.83268	6.8	Colica et al., 2019
TS1_20	**TS1**	Soil	42.78489	11.74136	63	Fornasaro et al., 2022a
TS1_21	**TS1**	Soil	42.78428	11.74116	56	Fornasaro et al., 2022a
TS1_22	**TS1**	Soil	42.78391	11.74158	30	Fornasaro et al., 2022a
TS1_23	**TS1**	Soil	42.78352	11.74115	11.4	Fornasaro et al., 2022a
TS1_1	**TS1**	Soil	42.78782	11.74536	0.83	Rimondi et al., 2019
TS1_10	**TS1**	Soil	42.78624	11.74384	86	Rimondi et al., 2019
TS1_11	**TS1**	Soil	42.78600	11.74368	53	Rimondi et al., 2019
TS1_12	**TS1**	Soil	42.78581	11.74354	37	Rimondi et al., 2019
TS1_13	**TS1**	Soil	42.78561	11.74325	7.2	Rimondi et al., 2019
TS1_14	**TS1**	Soil	42.78553	11.74311	3.5	Rimondi et al., 2019
TS1_15	**TS1**	Soil	42.78528	11.74281	3.2	Rimondi et al., 2019
TS1_16	**TS1**	Soil	42.78524	11.74259	4.8	Rimondi et al., 2019
TS1_17	**TS1**	Soil	42.78502	11.74201	26	Rimondi et al., 2019
TS1_18	**TS1**	Soil	42.78489	11.74195	22	Rimondi et al., 2019
TS1_19	**TS1**	Soil	42.78471	11.74188	33	Rimondi et al., 2019
TS1_2	**TS1**	Soil	42.78769	11.74524	5.7	Rimondi et al., 2019
TS1_3	**TS1**	Soil	42.78756	11.74507	12	Rimondi et al., 2019
TS1_4	**TS1**	Soil	42.78744	11.74487	73	Rimondi et al., 2019
TS1_5	**TS1**	Soil	42.78730	11.74473	78	Rimondi et al., 2019
TS1_6	**TS1**	Soil	42.78709	11.74449	120	Rimondi et al., 2019
TS1_7	**TS1**	Soil	42.78690	11.74427	17.6	Rimondi et al., 2019
TS1_8	**TS1**	Stream sediment	42.78664	11.74403	70	Rimondi et al., 2019
TS1_9	**TS1**	Soil	42.78647	11.74395	56	Rimondi et al., 2019
TS2_1	**TS2**	Soil	42.79654	11.80089	90	Colica et al., 2019
TS2_2	**TS2**	Soil	42.79593	11.80005	182	Colica et al., 2019
TS2_3	**TS2**	Soil	42.79565	11.79977	79	Colica et al., 2019
TS2_4	**TS2**	Stream sediment	42.79527	11.79946	29.4	Colica et al., 2019
TS2_5	**TS2**	Soil	42.79498	11.79899	76.4	Colica et al., 2019
TS2_6	**TS2**	Soil	42.79477	11.79856	185.5	Colica et al., 2019

TS2_7	**TS2**	Soil	42.79457	11.79815	94	Colica et al., 2019
TST_1	**TST**	Soil	42.74606	11.76313	0.7	Rimondi et al., 2019
TST_10	**TST**	Soil	42.74447	11.76186	13.8	Rimondi et al., 2019
TST_11	**TST**	Soil	42.74422	11.76157	10.7	Rimondi et al., 2019
TST_12	**TST**	Soil	42.74411	11.76138	<0.2	Rimondi et al., 2019
TST_13	**TST**	Soil	42.74406	11.76132	0.23	Rimondi et al., 2019
TST_14	**TST**	Soil	42.74400	11.76120	0.45	Rimondi et al., 2019
TST_2	**TST**	Soil	42.74585	11.76302	5.1	Rimondi et al., 2019
TST_3	**TST**	Soil	42.74568	11.76297	1.83	Rimondi et al., 2019
TST_4	**TST**	Soil	42.74534	11.76301	7.2	Rimondi et al., 2019
TST_5	**TST**	Soil	42.74516	11.76277	20	Rimondi et al., 2019
TST_6	**TST**	Stream sediment	42.74503	11.76274	16.55	Rimondi et al., 2019
TST_7	**TST**	Soil	42.74500	11.76246	23	Rimondi et al., 2019
TST_8	**TST**	Soil	42.74487	11.76233	19	Rimondi et al., 2019
TST_9	**TST**	Soil	42.74486	11.76188	11.6	Rimondi et al., 2019

473 *Tab. S1 Location, Hg concentration (mg/kg), and reference of the collected soils and stream*
474 *sediments along transects.*

Declaration of interests

☒The authors declare that they have no known competing financial interests or personal relationships that could have appeared to influence the work reported in this paper.

☐The authors declare the following financial interests/personal relationships which may be considered as potential competing interests: